Supplementary Information for

Modulating multivalent ion interaction in angstrom-scale confinement through solvent environment

by Xiaolin Yue et al.

This PDF file includes:

Supplementary Note

Definition of enrichment factor

Enrichment factor of an element in mixed uptake is defined as:

$$\text{Enrichment factor (EF)}_i = \frac{(C_i^{memb} / \sum_j C_j^{memb})}{(C_i^{feed} / \sum_j C_j^{feed})}$$

where

- C_i^{memb} is molar fraction of element *i* in the membrane after uptake,
- C_i^{feed} is initial concentration of element *i* in the feed solution,
- $\sum_j C_j^{memb}$ and $\sum_j C_j^{feed}$ are concentration (or molar fraction) of the other elements *j* in the membrane and feed, respectively.

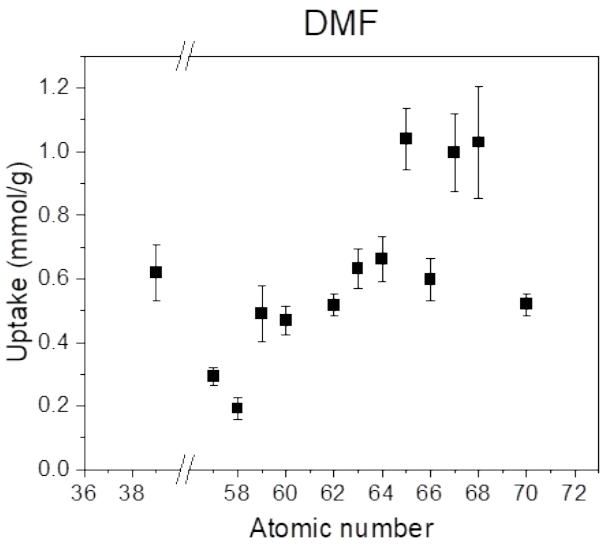

Fig. S1 Single ion uptake of MoS_2-COOH membrane in DMF solvent. Uptake condition: 3 mL of 50 mM single salt solution, mass loading of MoS_2-COOH membrane ~0.3 mg, uptake for 3 days.

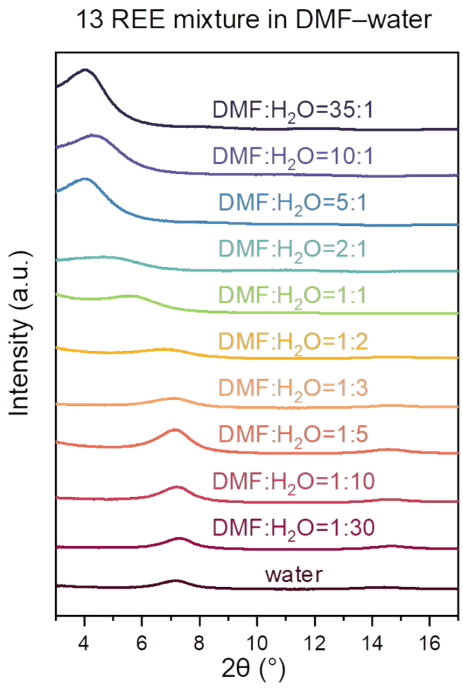

Fig. S2 XRD spectra of MoS_2-COOH membrane in 13 REE mixtures at various DMF–water molar ratios. The concentration of mixture solution is 5 mM for each REE cation.

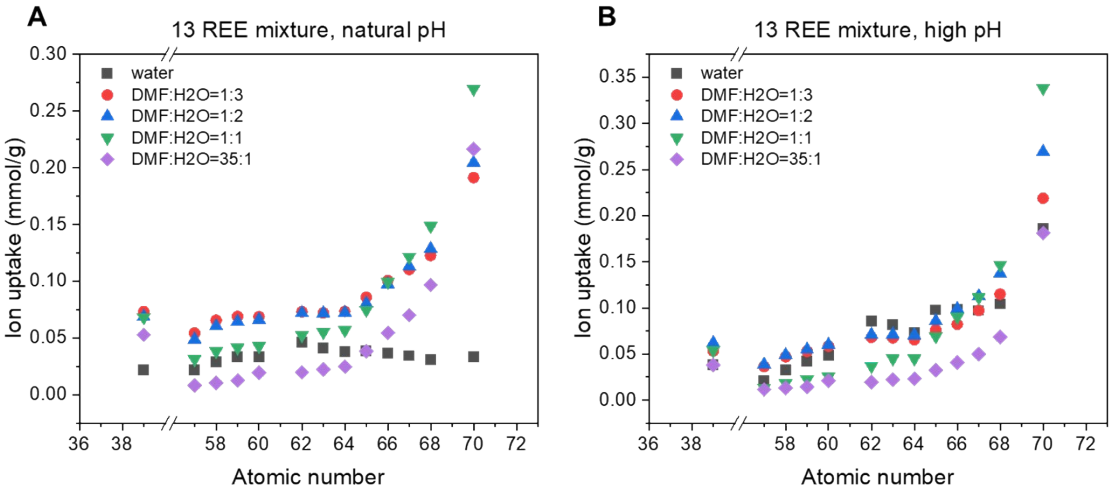

Fig. S3 pH effect of ion uptake in DMF–water mixtures in MoS_2-COOH membrane. The concentration of 13 REE mixture solution is 5 mM for each cation. Natural pH refers to the initial pH when salts are dissolved in the solvent, while high pH condition was achieved by adding concentrated potassium hydroxide (KOH) solution. Note that the upper pH limit is constrained by the Ksp of REE hydroxides precipitation. In aqueous solutions, the natural pH of the REE mixture is ~4.1, and high pH is adjusted to ~6.5.

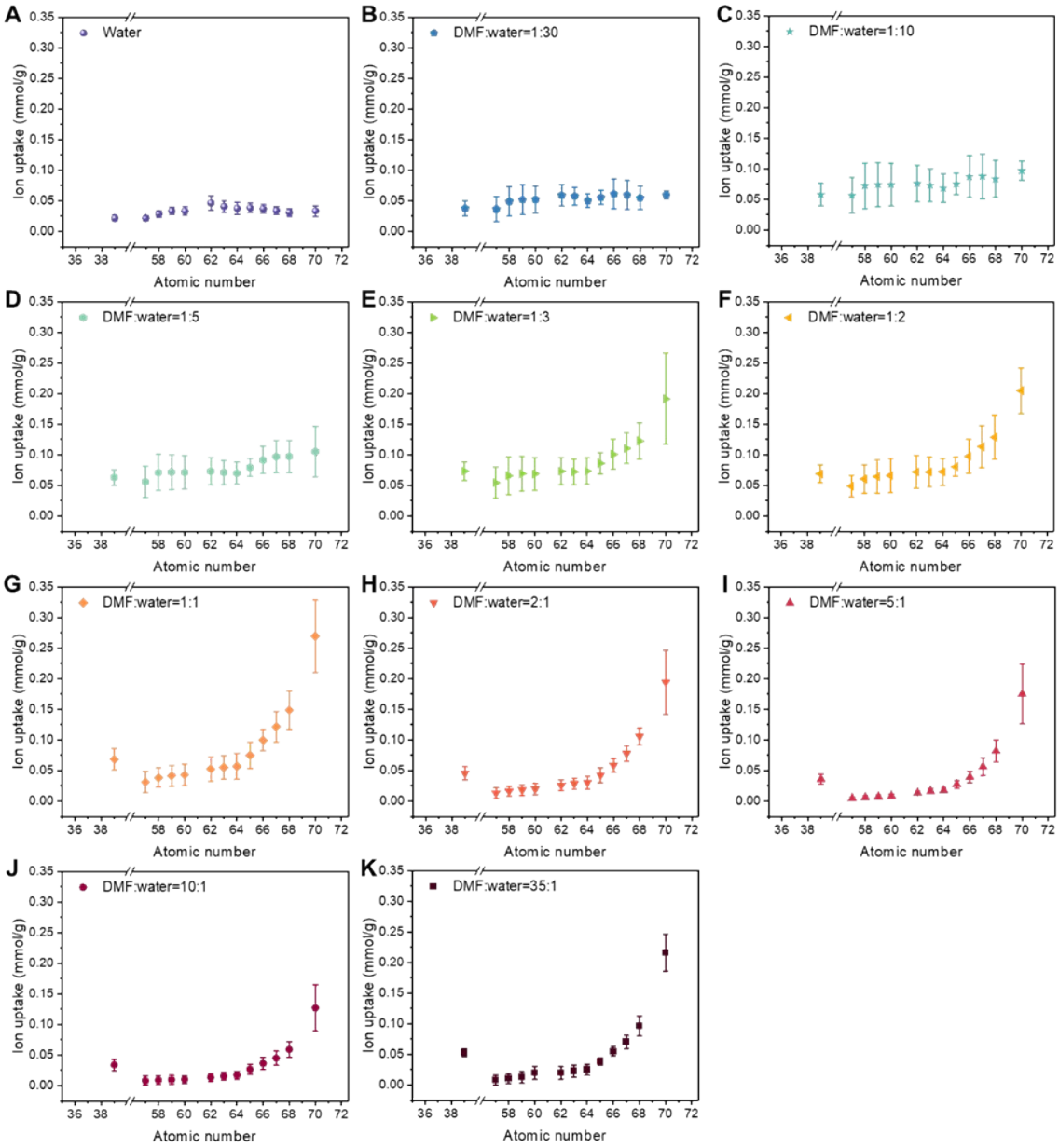

Fig. S4 Ion uptake of each element in 13 REE mixtures at various DMF–water molar ratios. (A–K) correspond to DMF–water molar ratios of 0, 1:30, 1:10, 1:5, 1:3, 1:2, 1:1, 2:1, 5:1, 10:1, and 35:1, respectively.

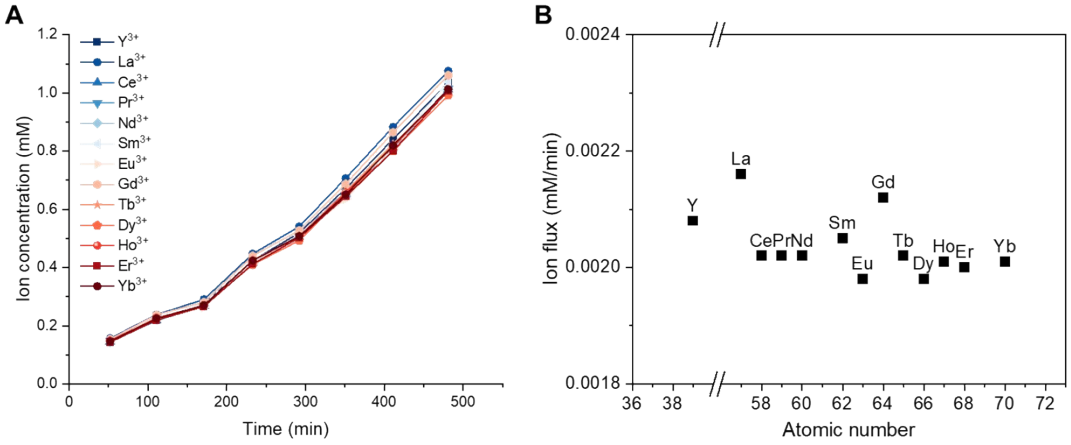

Fig. S5 REE cations transport across MoS_2-COOH/PTFE membrane in DMF. The feed solution is 13 REE mixture in DMF (5 mM for each cation), while the permeate is pure DMF. (A) Ion concentration profiles for REE ion in the permeate. (B) Permeability of the REE ion in DMF across MoS_2-COOH/PTFE membrane.

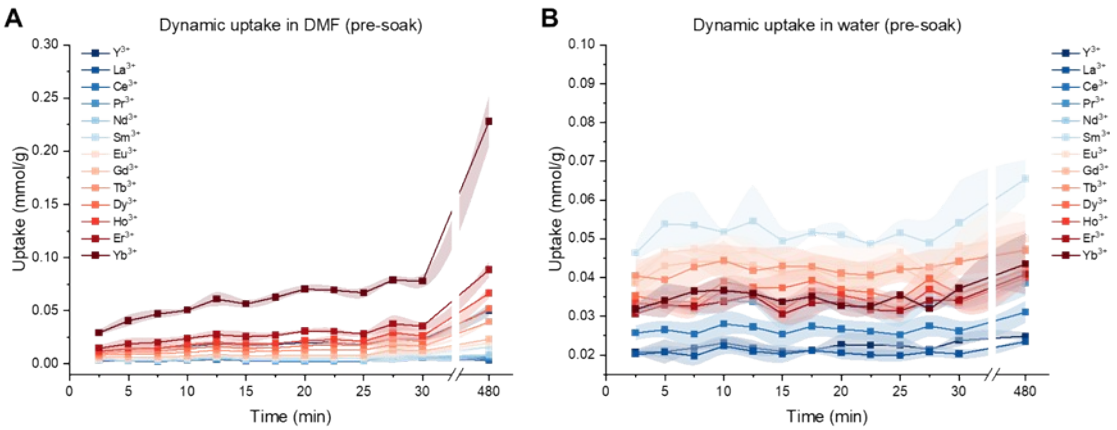

Fig. S6 Dynamic uptake of 13 REE mixture with pre-soaked membranes. (A) Time-dependent uptake in DMF with membranes pre-soaked in DMF. (B) Time-dependent in water with membranes pre-soaked in water. The concentration of 13 REE mixture is 5 mM for each REE ion. Error bars represent the standard deviation from two independent tests.

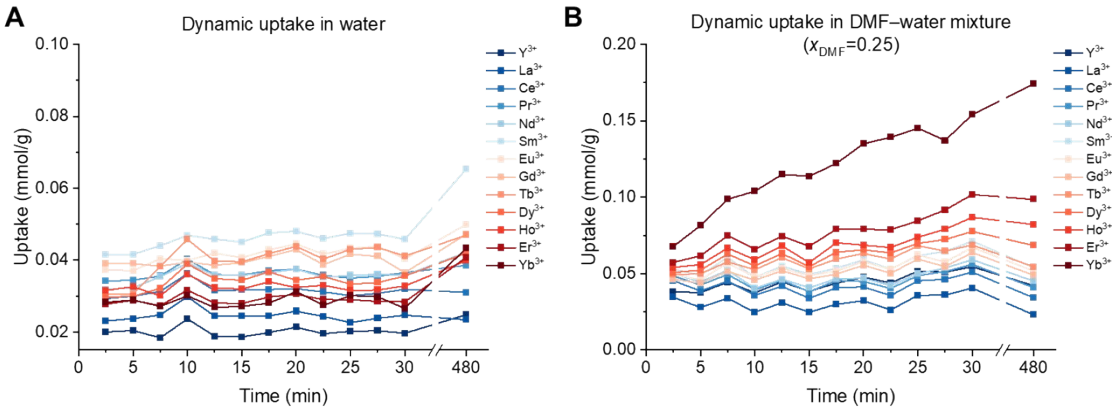

Fig. S7 Dynamic uptake of 13 REE mixture. (A) Time-dependent uptake in water. (C) Time-dependent uptake in DMF–water mixture at x_{DMF} = 0.25. The above dynamic uptake tests were carried out without the pre-soak step. The concentration of 13 REE mixture is 5 mM for each REE ion.

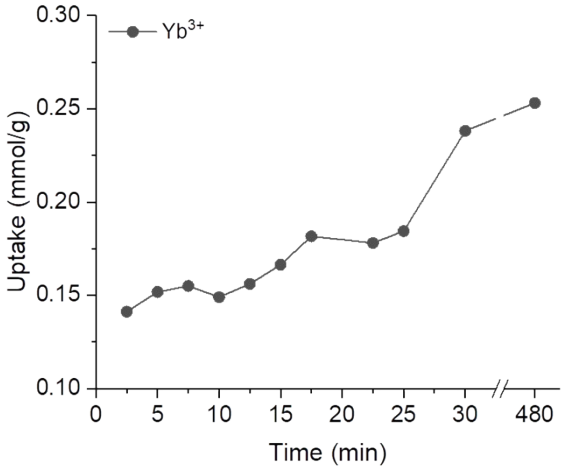

Fig. S8 Time-dependent uptake of single Yb ion solution in DMF. The uptake test was carried out without the pre-soak step. The concentration of single Yb ion solution is 50 mM.

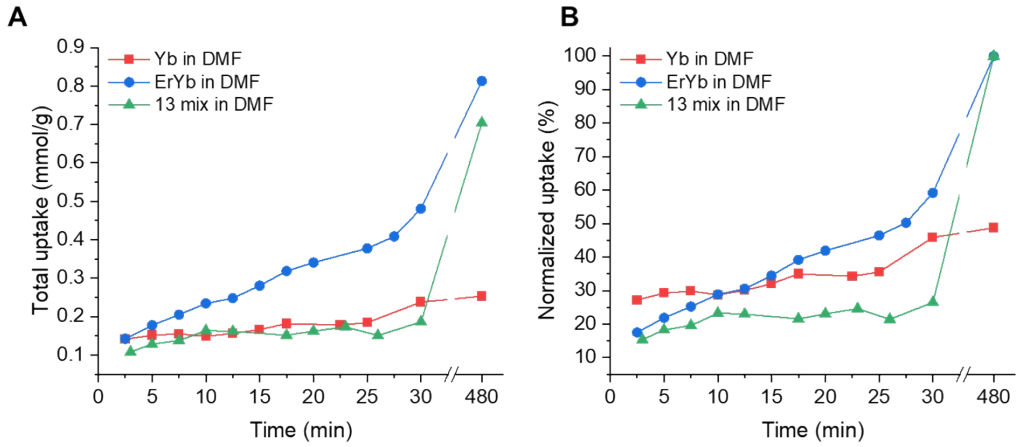

Fig. S9 Dynamics of total uptake in DMF. (A) Time evolution of absolute total uptake amount. (B) Time evolution of total uptake normalized to its final value. For the binary Er–Yb system and the 13 REE mixture, the uptake values are normalized to the amount at 8 hours (480 min). The single Yb ion results are normalized to the corresponding single ion uptake shown in Fig. S1.

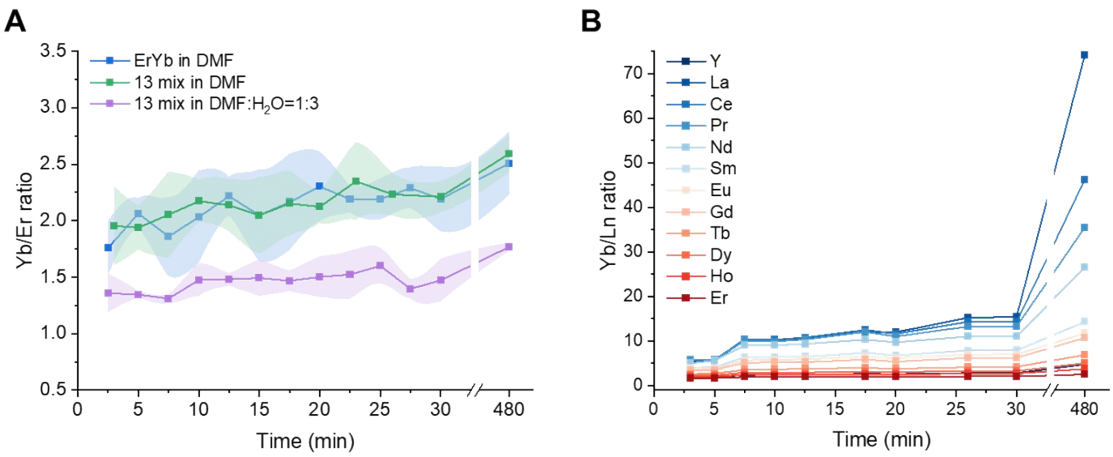

Fig. S10 Dynamics of Yb ion selectivity. (A) Dynamics of Yb selectivity quantified by Yb/Er ratio. Error bars represent the standard deviation from two independent tests. (B) Dynamics of Yb/Ln ratio in 13 REE mixture in DMF. Ln denotes all other REEs except Yb (Ln = Y, La, Ce, Pr, Nd, Sm, Eu, Gd, Tb, Dy, Ho, Er).

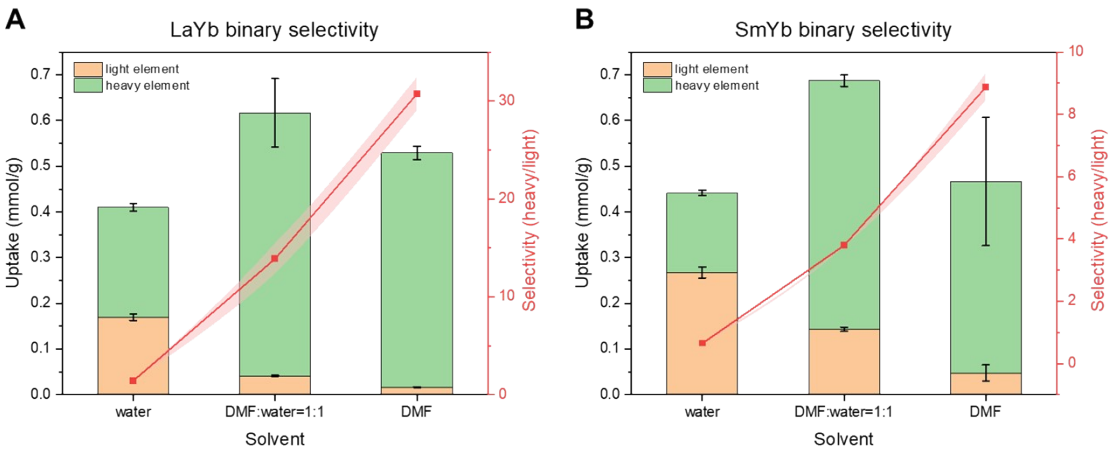

Fig. S11 Yb uptake selectivity in binary mixtures with varying DMF content. Uptake amount and binary selectivity of Yb/La (A) and Yb/Sm (B) in water, DMF–water mixture at 1:1 molar ratio, and DMF. Error bars represent the standard deviation from three independent uptake tests.

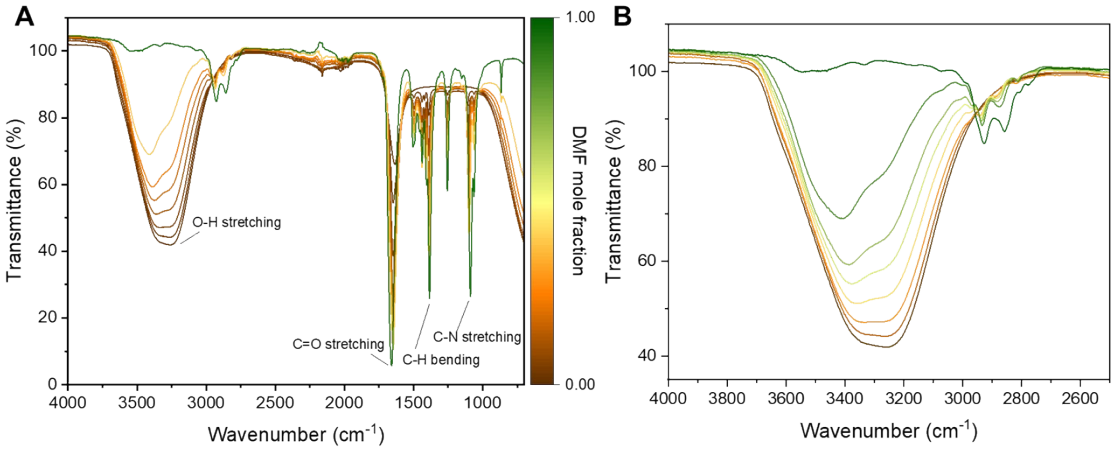

Fig. S12 Fourier transform infrared (FTIR) spectroscopy of DMF–water solvent mixtures at varying composition ratios. (A) Full FTIR spectra. (B) Close-up view of the O–H stretching region. The FTIR data show a clear trend: as DMF fraction increases, the O–H stretching band shifts to higher wavenumbers (blue shift), indicating stronger O–H bonds and a weaker hydrogen bonding network.

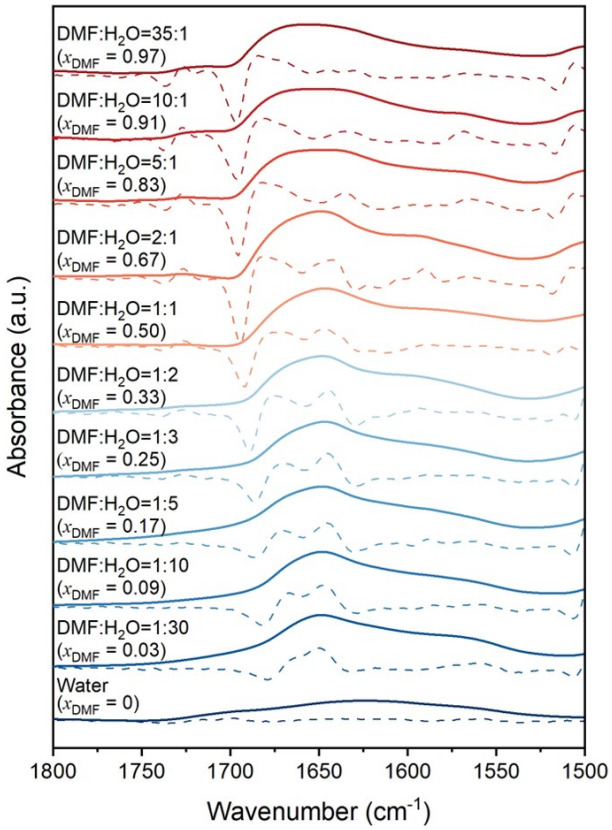

Fig. S13 Effect of DMF fraction on attenuated total reflectance FTIR (ATR-FTIR) spectra of wet MoS_2-COOH membranes. Solid lines show the absorption spectra, while the dashed lines represent the corresponding negative second-order derivatives for peak identification. Prior to measurement, excess solvent was removed from the membrane surface while preserving the confined solvent within channels.

Note:

Analysis of the negative second-order derivative spectra reveals two distinct derivative peaks with different peak positions, indicating that the observed C=O stretching envelope is composed of at least two overlapping contributions from carbonyl groups in different local environments. The lower-wavenumber derivative peak is attributed to carbonyl groups experiencing stronger hydrogen bonding or coordination interactions. Such interactions weaken the C=O bond, resulting in a red-shifted vibrational frequency. In contrast, the higher-wavenumber derivative peak corresponds to more weakly interacting carbonyl groups and thus stronger C=O bonds.

In the water-rich regime ($x_{DMF} \leq 0.25$), the lower-wavenumber peak is more prominent in the derivative spectra. This indicates stronger curvature of the absorbance band associated with carbonyl groups experiencing strong hydrogen-bonding interactions, which dominate the local vibrational response. This observation is consistent with XRD results (Fig. 2A) showing that the interlayer spacing remains similar to that in pure water, suggesting that DMF is incorporated into the channels while preserving the overall water-like solvent structure, likely by replacing certain solvation sites without significantly altering the channel geometry. At intermediate DMF fractions (x_{DMF} = 0.33 and 0.50), the two derivative peaks are comparable, marking a

distinct transition point that coincides with the expansion in interlayer spacing. This reflects a redistribution of DMF coordination environments as DMF molecules increasingly populate the channels, with a growing contribution from more weakly hydrogen-bonded or less coordinated DMF configurations. Under DMF-rich conditions ($x_{DMF} \geq 0.67$), the higher-wavenumber derivative peak undergoes a pronounced blue shift of approximately 10 cm^{-1}, reaching over 1680 cm^{-1}, and becoming more prominent in the derivative spectra. This shift indicates a stronger C=O bond and a weaker coordination environment of DMF, mainly with REE ions. The observation aligns with the observed decrease in total DMF uptake, with fewer REE ions available for coordination and therefore reduced DMF–REE interactions. Overall, these results reveal a composition-dependent evolution of the confined DMF environment, from water-like structures at low DMF fractions, to a regime of weakened DMF–REE interactions at high DMF fractions consistent with a decrease in uptake.

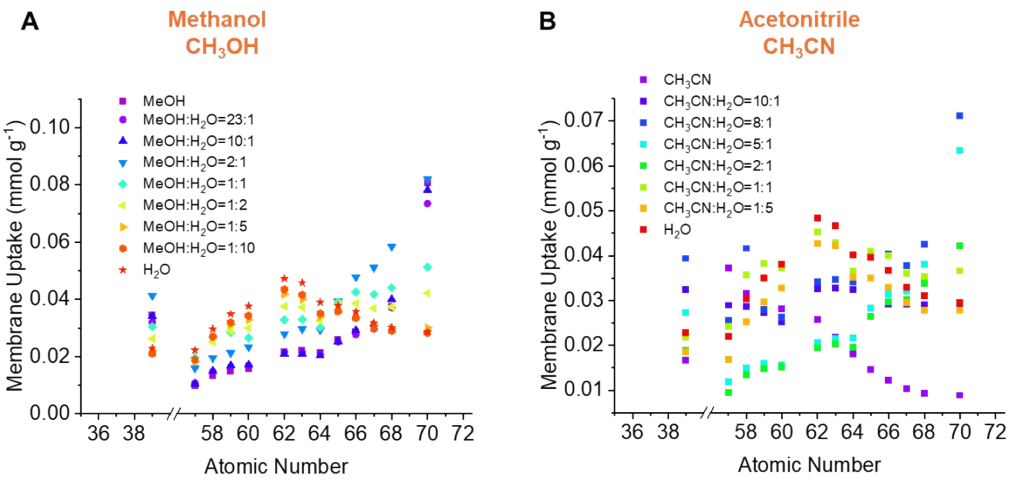

Fig. S14 Ion uptake of 13 REE mixtures at various solvent compositions in MoS_2-COOH membrane. (A) Methanol-based system. (B) Acetonitrile-based system.

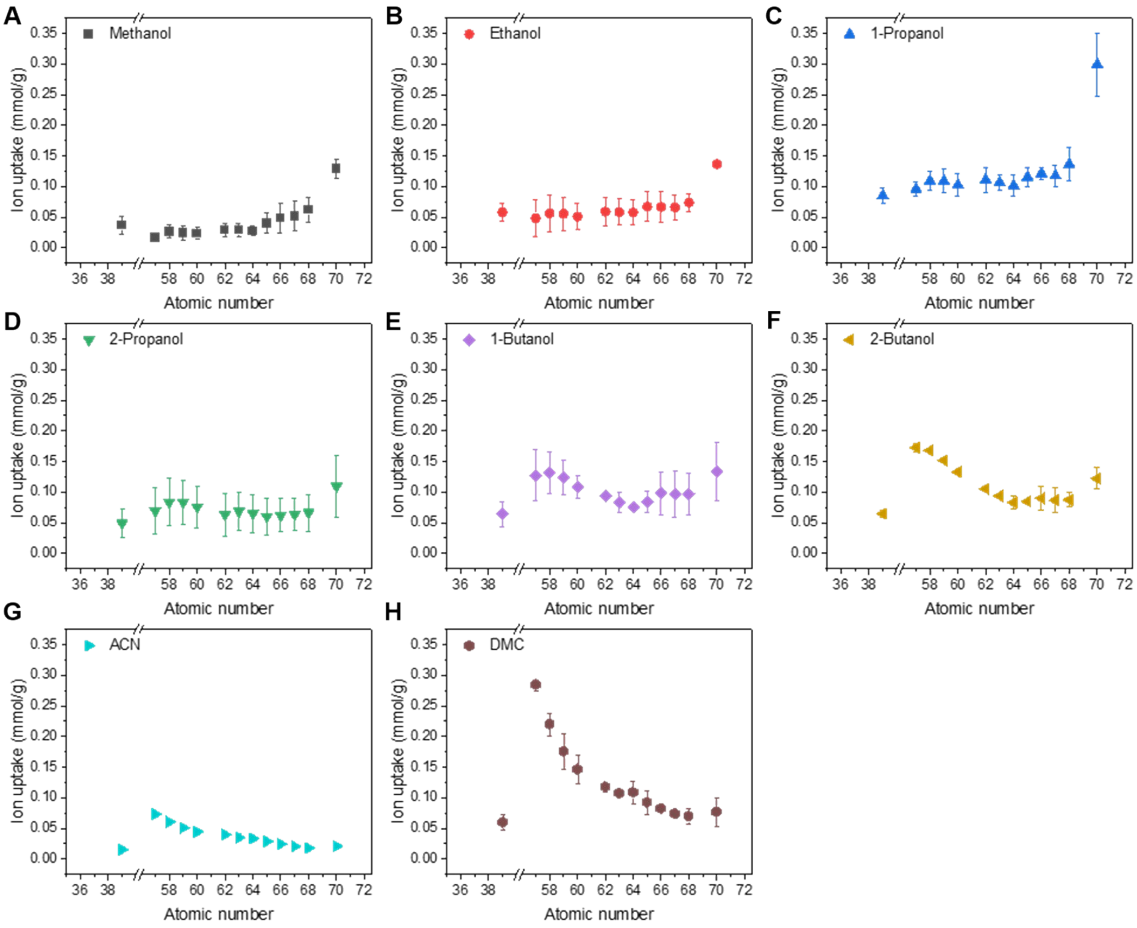

Fig. S15 Ion uptake of each element in 13 REE mixtures across solvent environments. (A–H) correspond to methanol, ethanol, 1-propanol, 2-propanol, 1-butanol, 2-butanol, acetonitrile (ACN), and dimethyl carbonate (DMC). Error bars represent the standard deviation from at least two independent tests.

Table S1 Experimental dielectric constant and Hammett acidity function (H_0) for DMF–water mixtures

DMF:H_2O molar ratio	DMF mole fraction	Dielectric constant (25°C)	H_0
35:1	0.9722	39.98	20.88
10:1	0.9091	40.44	20.34
5:1	0.8333	41.81	19.69
2:1	0.6667	46.57	18.26
1:1	0.5000	51.15	16.83
1:2	0.3333	57.91	15.40
1:3	0.2500	63.77	14.68
1:5	0.1667	69.28	13.97
1:10	0.0909	74.97	13.32
1:30	0.0323	76.40	12.81
0	0.0000	79.50	12.54

Note: (i) The experimental dielectric constants are obtained from Ref. 32, which reports the static dielectric constant at various DMF volume fraction. Values at intermediate compositions were obtained by linear interpolation.

(ii) The Hammett acidity functions are obtained from Ref. 34, where the H_0 values were measured for DMF–water mixtures containing 0.019 M tetramethylammonium hydroxide. For DMF mole fraction larger than 70%, the values were from extrapolation of the literature data.